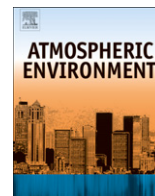




Contents lists available at ScienceDirect

Atmospheric Environment

journal homepage: www.elsevier.com/locate/atmosenv

Carbon dioxide fluxes over an urban park area

Klaus Kordowski*, Wilhelm Kuttler¹

Department of Applied Climatology and Landscape Ecology, Institute of Geography, University of Duisburg-Essen, Campus Essen, D-45127 Essen, Germany

ARTICLE INFO

Article history:

Received 11 February 2010

Received in revised form

21 April 2010

Accepted 21 April 2010

Keywords:

Carbon dioxide

Flux

Essen

Germany

Urban surface

Park

Eddy covariance

Artificial neural networks

ABSTRACT

From September 2006 to October 2007 turbulent fluxes of carbon dioxide were measured at an urban tower station (26 m above ground level, $z/z_h = 1.73$) in Essen, Germany, using the eddy covariance technique. The site was located at the border between a public park area (70 ha) in the south–west of the station and suburban/urban residential as well as light commercial areas in the north and east of the tower. Depending on the land-use two different sectors (*park* and *urban*) were identified showing distinct differences in the temporal evolution of the surface–atmosphere exchange of CO₂. While urban fluxes appear to be governed by anthropogenic emissions from domestic heating and traffic (average flux 9.3 $\mu\text{mol m}^{-2} \text{s}^{-1}$), the exchange of CO₂ was steered by biological processes when the park contributed to the flux footprint. The diurnal course during the vegetation period exhibited negative daytime fluxes up to $-10 \mu\text{mol m}^{-2} \text{s}^{-1}$ on average in summer. Nevertheless, with a mean of 0.8 $\mu\text{mol m}^{-2} \text{s}^{-1}$ park sector fluxes were slightly positive, thus no net carbon uptake by the surface occurred throughout the year.

In order to sum the transport of CO₂ a gap-filling procedure was performed by means of artificial neural network generalisation. Using additional meteorological inputs the daily exchange of CO₂ was reproduced using radial basis function networks (RBF). The resulting yearly sum of 6031 $\text{g m}^{-2} \text{a}^{-1}$ indicates the entire study site to be a considerable source of CO₂.

© 2010 Elsevier Ltd. All rights reserved.

1. Introduction

To analyse and predict recent and future climate change on a global scale exchange processes of greenhouse gases – primarily carbon dioxide (CO₂) – over various ecosystems are of rising interest. In order to upscale land-use dependent sources and sinks of CO₂, knowledge of the local variability of carbon fluxes is needed. Among terrestrial ecosystems urban areas play an important role because most of anthropogenic emissions of carbon dioxide originate from these areas (Svirejeva-Hopkins et al., 2004). In 2006 the degree of urbanisation of the world's population reached 50% (UN-Habitat, 2006) which emphasises the need for a reliable data basis of exchange processes over populated and built-up surfaces.

The eddy covariance technique (EC) is a widely used tool to measure turbulent fluxes of mass, heat and momentum at the earth–atmosphere interface. Its application over vegetated surfaces emerged rapidly over the last two decades (Baldocchi, 2003) and there were networks developed measuring fluxes of CO₂ worldwide over various ecosystems (e.g. FLUXNET: Baldocchi et al., 2001,

Baldocchi, 2008; Papale et al., 2006). The use of EC in urban boundary layer studies for measuring trace gas fluxes is still emerging and the number of publications regarding reliable information about the exchange of carbon dioxide over densely populated areas is limited.

Turbulent fluxes usually are measured at some height above ground within the constant flux layer (CFL) to evaluate the surface–atmosphere exchange for a specific area around the site. However, this so called flux footprint (e.g. Schmid, 2002; Vesala et al., 2008b) can be variable according to the type of surface cover contributing to the flux. Considering that surfaces can be sources or sinks in terms of carbon exchange, this evaluation can be challenging especially in urban areas due to increased heterogeneity at some sites.

In general, the exchange of CO₂ over cities is mostly governed by anthropogenic emissions originating from road traffic and local heating with natural gas, oil or coal (Table 1). This results in positive fluxes of CO₂, i.e. the transport is directed into the atmosphere throughout the day (e.g. Grimmond et al., 2002; Moriwaki and Kanda, 2004). Maximum emissions are reported to occur daytimes with peak values during rush hours. The impact of vehicle emissions on the flux was also indicated by correlations with traffic counts in several studies (Velasco et al., 2005; Matese et al., 2009; Soegaard and Møller-Jensen, 2003).

However, observations at sites whose surrounding is characterised by a high portion of urban vegetation show evidence for

* Corresponding author. Tel.: +49 (0) 201 183 2723; fax: +49 (0) 201 183 3239.

E-mail addresses: klaus.kordowski@uni-due.de (K. Kordowski), wilhelm.kuttler@uni-due.de (W. Kuttler).¹ Tel.: +49 (0) 201 183 2734; fax: +49 (0) 201 183 3239.

Table 1
List of urban studies dealing with EC measurements of CO₂ fluxes.

Authors	Location	Site characteristics	Height ^a (z/z _h)	Duration	F _c ^b (μmol m ⁻² s ⁻¹)	
					Min	Max
Matese et al., 2009	Florence, Italy	urban	1.3	108 d	9	41
Schmidt et al., 2008	Münster, Germany	urban	z = 65 m	43 d	4	11
Vesala et al., 2008a	Helsinki, Finland	suburban	1.6	0.75 a	-4	35
Coutts et al., 2007	Melbourne, Australia	urban/suburban	2	1 a	2	11
Vogt et al., 2006	Basel, Switzerland	urban	0.1–2.1	30 d	3	16
Velasco et al., 2005	Mexico City, Mexico	suburban	3	23 d	3	18
Grimmond et al., 2004	Marseille, France	urban	1.8–2.8	28 d	0	30
Soegaard and Møller-Jensen, 2003	Kopenhagen, Denmark	urban	1.7	1 a	5	36
Moriwaki and Kanda, 2004	Tokyo, Japan	suburban	3.9	1 a	5	25
Nemitz et al., 2002	Edinburgh, Scotland	urban/suburban	z = 35 m	32 d	10	38
Grimmond et al., 2002	Chicago, USA	suburban	4.2	48 d	0	10

^a If no z/z_h is given by the authors, measuring height above ground level (z) is presented.

^b Minimum and maximum values of F_c are based on average diurnal variations presented in the publications.

effects of biological processes on the flux. At daytimes during summer the uptake of CO₂ caused by photosynthetic plant activity may lead to an offsetting of positive fluxes (Coutts et al., 2007). Night-time carbon exchange is described to be governed by plant and soil respiration at rural sites (e.g. Goulden et al., 1996) but there are also some indications for an impact of these processes on the dynamics of CO₂ within the urban environment (Ptak and Kuttler, submitted for publication).

At sites where the land-use properties in certain wind direction sectors differ in terms of vegetation cover and/or source strengths, distinct differences in the temporal evolution of CO₂ fluxes have been found between those sectors. In case of flux footprints including larger green spaces even negative fluxes in average at noon during spring and summer have been observed (Vesala et al., 2008a).

These findings underline the potential of parks and vegetated spaces within cities for sequestering carbon due to the above- and below ground plant biomass build-up. Most of the studies dealing with carbon uptake of urban vegetation are based on inventories of the vegetation stand. For example, McPherson (1998) estimated an annual sequestration of 1.2 t CO₂ ha⁻¹ a⁻¹ by the urban forests of Sacramento, CA (USA) while Nowak and Crane (2002) extrapolated data of 10 US-cities to the national scale and found an average annual uptake of 2.9 t CO₂ ha⁻¹ a⁻¹.

In summary a unique pattern of urban CO₂ fluxes cannot be drawn. Beside the observation that all examined areas act as net sources of CO₂ due to anthropogenic emissions, diurnal and annual characteristics vary between different sites indicating the flux to be a product of both, anthropogenic and biogenic factors. Consequently the advantage of applying EC is the direct assessment of integrated surface exchanges in terms of a top-down approach.

The purpose of this study is to quantify the turbulent flux of carbon dioxide over a park area embedded in an urban/suburban surrounding for a time period of an entire vegetation period to analyse the temporal evolution on both, the daily and seasonal scale. Based on a continuous 14 month flux dataset the question should be answered whether the vegetated area has the ability to act as a local sink for CO₂ and to what extend local sinks might influence the total carbon exchange at the site.

2. Materials and methods

2.1. Study site and surface characteristics

The measurements were carried out over a time period of nearly 14 months from September 2006 to October 2007 in Essen, Germany. The city with 580,000 inhabitants (2007) covers a surface area of 210 km² and is located in the western part of Germany.

It marks the southern part of the Ruhr metropolitan area, a high density urban agglomeration with about 5.2 million inhabitants. The study site was located at a distance of about 3 km to the south–west from the city centre at the border between an urban park in the south–west of the site and suburban/urban residential areas to the east and north (Fig. 1).

A solid concrete tower, actually a visitor look-out, hosted the equipment for the flux measurements (51° 25.839' N, 6° 59.536' E, 111 m asl, below denoted as GRT). At a height of 26 m above ground level (agl) the instrumentation was mounted on a horizontal boom. It extended 3.5 m from the tower to the south–east assuring minimal flow distortion by the building with respect to the predominant wind directions from south–west and north–east respectively (i.e. the tower is situated upwind of the instrumentation for a minimum of time; cf. Section 3.1). At the height of the boom the tower building measures 5.2 × 3.6 m with the longer side orientated in E–W direction.

According to the land-use differences around the site as depicted in Fig. 1, two sectors will be regarded separately within this paper (Table 2): On the one hand the **urban sector** to the east of the tower (0° < φ ≤ 180°), on the other hand the **park sector** in the south–west (180° < φ ≤ 270°). In case of winds coming from north–west (270° < φ < 360°) the tower building is situated upwind; the according data was excluded from the dataset for reasons of quality assurance (cf. Section 2.1).

The area of the park to the south–west of the tower covers 70 ha with a plant inventory consisting mainly of broadleaf vegetation and lawns. It adjoins several smaller forest patches outside the park in the west (mainly European beech) resulting in a vegetated area with a total size of ≈90 ha. At a distance of 1 km to the west of the tower residential housings are located which are characterised by a high fraction of gardens and urban vegetation. The ratio of vegetated area to the total area (vegetation plane area density λ_v) has been derived from aerial photographs using a colour filter technique. The ratio of built-up surfaces to the total area (λ_b) was calculated using the land-use scheme shown in Fig. 1. It was found λ_v = 0.52 and λ_b = 0.12 on average in the **park sector**. Both holds for a 1 km circle around the tower site. For the same range a mean obstacle height (tree stands and buildings) of about z_h = 12 m was estimated. A road with light traffic (≈1000 veh d⁻¹) crosses the park from east to west.

On the opposite, land-use within the **urban sector** is of typical suburban/urban characteristics. Surface cover mainly consists of dense residential and light commercial areas with buildings of 2–4 floors (z_h = 15 m). In the south–east of the site an exhibition centre is situated with several larger buildings of the same height. Despite the high building density within the **urban sector** (λ_b = 0.59) a significant fraction of urban vegetation is apparent (λ_v = 0.22).

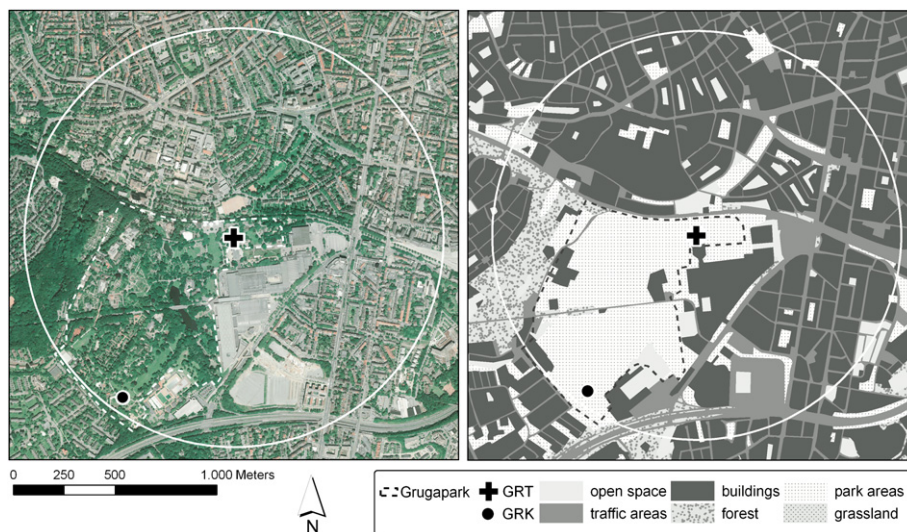


Fig. 1. Aerial photograph of the area around the measurement site (left), land-use classification for the same area (right). The location of the measurement tower (GRT) is indicated by the black cross; the black dot shows the meteorological station GRK. The circle indicates a radius of 1 km around the tower. Note that the station HSW is situated outside the map.

Furthermore this area is characterised by several main roads of high traffic intensity. In total the average daily amount vehicle kilometres travelled was estimated to be $184 \times 10^3 \text{ km d}^{-1}$ for the urban sector (in contrast to only $26 \times 10^3 \text{ km d}^{-1}$ for the park sector; estimations based on data provided by the local authorities).

In order to perform footprint calculations (cf. 3.2.) values for the surface roughness z_0 were derived anemometrically by transformation of the vertical wind profile's log-law using measured data. The displacement height d was estimated as $d = 0.66 z_h$ (e.g. Grimmond and Oke, 1999, Table 3).

Additional meteorological measurements were carried out at sites within the adjacency of GRT: Air temperature, relative humidity, wind speed and direction were measured at 2 m agl at a site within the park, situated at a distance of 800 m to GRT (GRK, cf. Fig. 1). Data for shortwave irradiance and precipitation were taken from the rural site Harscheidweg (HSW) at a distance of 3.3 km from GRT to the south–west.

2.2. Instrumentation and data treatment

The tower site was equipped with a sonic anemometer-thermometer (USA-1, Metek, Germany) sampling horizontal and vertical wind vectors u , v , w and acoustic temperature (t_s). CO_2 and H_2O molar densities were measured with a non-dispersive infrared open-path analyser (LI 7500, Li-Cor Biosciences, USA). Both instruments have been operated at a sampling frequency of 10 Hz. From raw data 30 min block averages and covariances were calculated for

Table 2

Overview of the measurement sites and equipment. u , v , w indicate the wind vectors, t_s the sonic temperature, ρ_c and ρ_v the molar densities of CO_2 and water vapour respectively, t_a the air temperature, U the wind speed, ϕ the wind direction, S_d the solar radiation and P denotes precipitation.

Site	Latitude Longitude	Height (agl)	Quantity	Manufacturer (Model)	Sampling interval
GRT	51°25.563' N 6°59.563' E	26 m	u , v , w , t_s	Metek, GER (USA-1)	10 Hz
			ρ_c , ρ_v	Li-Cor, USA (LI 7500)	
GRK	51°25.456' N 6°59.129' E	2 m	t_a	Thies, GER (NTC)	1 s
			ϕ , U	Thies, GER (Cup, vane)	
HSW	51°25.181' N 6°59.878' E	2 m	S_d	Kipp & Zonen, NL (CMP 11)	1 s
			P	Friedrich, GER (Type 7501)	

subsequent analysis. The flux of carbon dioxide (F_c) in $\mu\text{mol m}^{-2} \text{s}^{-1}$ was calculated after.

$$F_c = \overline{w'\rho'_c} = \frac{1}{n-1} \sum_{k=0}^{n-1} [(w_k - \overline{w_k})(\rho_{ck} - \overline{\rho_{ck}})] \quad (1)$$

with w the vertical wind component in m s^{-1} and ρ_c the molar density of CO_2 in $\mu\text{mol m}^{-3}$. Data was rotated into streamwise coordinates using a double rotation procedure according to Kaimal and Finnigan (1994). Further steps of post-processing included the correction of temperature and water vapour density fluctuations according to Webb et al. (1980) and of high frequency spectral loss due to path length averaging and spatial separation of sensors (Moore, 1986). The cross wind correction was performed according

Table 3

Surface characteristics in a radius of 1 km around the study site divided into the different land-use sectors: *urban* to the east of the tower, *park* to the south–west (z is the measurement height above ground level, z_h the mean building height, z_0 the aerodynamic roughness length, d the displacement height). The stability parameter ζ and σ_v/u_* as a parameter for lateral turbulence intensity indicate the values used for initialising the flux footprint model FSAM.

Surface characteristic	URBAN $0^\circ < \phi \leq 180^\circ$	PARK $180^\circ < \phi \leq 270^\circ$
land-use	Residential, light commercial buildings, intense road traffic	Park area, few residential housings, little road traffic
z	26 m	26 m
z_h	15 m	12 m
z_0	1.35 m	1.07 m
d	10 m	8 m
z/z_h	1.73	2.05
λ_b^a	0.59	0.14
λ_v^b	0.22	0.52
road network length (km)	21.4	4.0
km travelled (10^3 km d^{-1}) ^c	184.2	26.6
$\zeta = (z-d)/L$	−0.05	−0.05
σ_v/u_*	1.99	1.88

^a Building area density: ratio of plan area of buildings to plan area of total surface.

^b Vegetation area density: ratio of area covered by vegetation to total area as derived from the aerial photograph (Fig. 1).

^c Based on data about the average daily traffic intensity provided by local authorities.

to Liu et al. (2001) with regard to the non-vertical sensor path of the USA-1 sonic.

Within the subsequent quality check fluxes which were measured under conditions of weak turbulent mixing were eliminated from the dataset by using a threshold for a minimum friction velocity with $u_* = 0.15 \text{ m s}^{-1}$. This accounted for 8.4% of the data.

The identification of low quality data due to precipitation, dust, pollen or other contamination on the sensor optics was carried out by an analysis of the LI 7500's *Active Gain Control* value (AGC) which was recorded parallel to the trace gas concentrations. In case of a sensor path disturbance this percentage value deviates from a standard and the particular dataset can be recognized as being of low quality.

This did not only affect times during precipitation but also led to a rejection of data for some time after precipitation events due to drops on the sensor window resulting in 21.4% of eliminated data during the study period.

To prevent the analysis of flux data influenced by interference and flow distortion caused by the tower building, data out of the wind direction sector $270^\circ < \phi < 360^\circ$ was rejected from the dataset. Another 6.6% of the data were filtered by this criterion. Overall, there were 63.8% of the measuring period (12,614 half hour blocks) available for further examination.

The stations GRK and HSW were equipped with standard meteorological instrumentation (Table 2). For all parameters recorded 3 min average values were available.

2.3. Gap-filling

In order to quantify the total annual exchange of carbon dioxide, a continuous time series is needed. Recently there have been manifold research activities regarding gap-filling strategies of EC data primarily at rural forests sites (Falge et al., 2001; Moffat et al., 2007). Many of them use empirical non-linear relationships between net fluxes and radiation and (soil) temperature respectively for filling data gaps. In heterogeneous urban environments the number of influencing factors contributing to the net exchange of CO_2 can be regarded as being too high for the formulation of simple regressions.

Artificial neural networks (ANN) are networks of interconnected simple processing units (neurons) and can be seen as simplified models of their biological archetypes. Due to their ability to recognize non-linear relations between variables, the application of artificial neural networks (ANN) for EC gap-filling is promising (Papale and Valentini, 2003; Moffat et al., 2007). The main issue of this approach is to train ANNs with data of (meteorological) variables related to the turbulent flux without describing empirical relationships. Particularly, radial basis function networks (RBF) were described as being superior to widely used multi-layer perceptron networks when applying them on urban flux data (Schmidt et al., 2008).

In this paper a gap-filling procedure with RBF networks was tested using the 14 month flux dataset and additional meteorological parameters. Networks were trained using the available flux data, time and meteorological parameters using back propagation of the networks' error. In a stepwise procedure the number of training variables was reduced based on their error ratio (cf. Schmidt et al., 2008). Thereby wind direction was fuzzy-transformed into four single values before starting the network training (cf. Table 4).

It turned out to be sufficient to use this wind direction data, air temperature and solar radiation as input values for the network to reproduce the fluxes with a lowest error. Solar radiation and temperature obviously exhibit enough time information for the temporal variability of anthropogenic emissions to 'code' flux

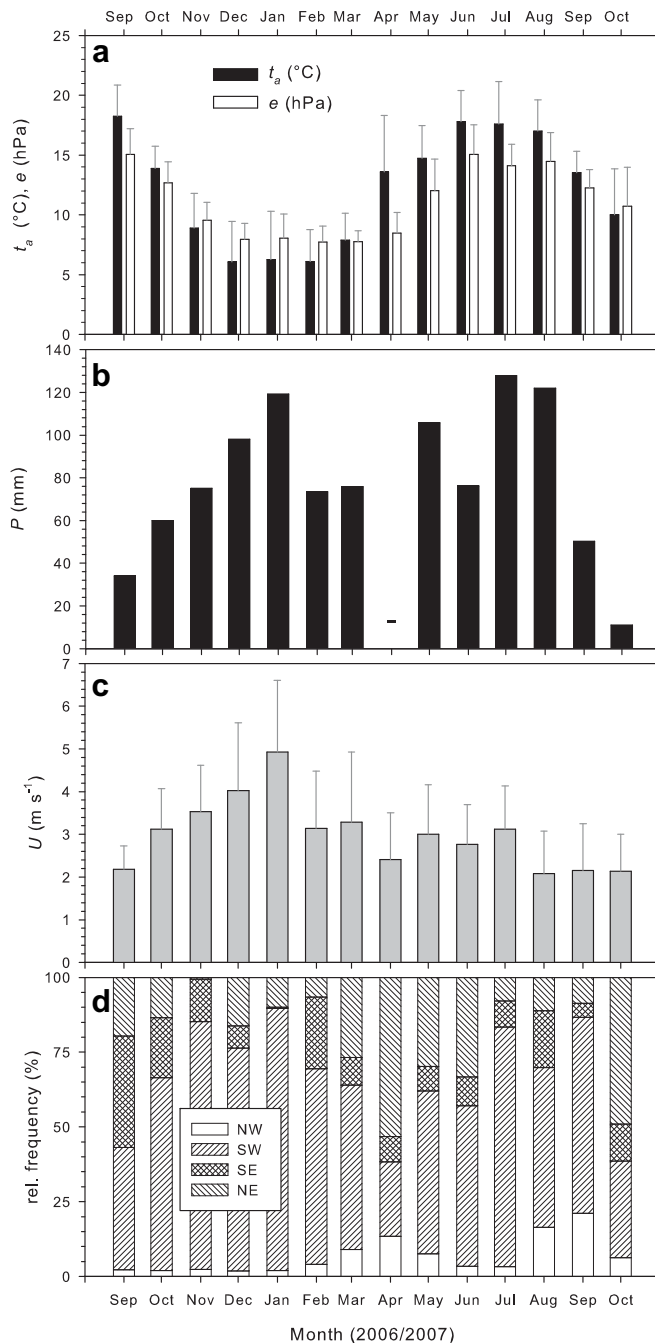


Fig. 2. Monthly values of meteorological quantities during the study period: (a) Average air temperature (t_a) and vapour pressure (e) at 2 m agl (GRK), (b) sums of precipitation (P) at HSW, (c) average wind speed (U) at 26 m agl (GRT), (d) relative frequency of wind direction out of 90°-sectors at GRT. All data is based on daily averages and sums; error bars indicate the single standard deviation. In April 2007 there has been no precipitation.

variations. Hence, it was not necessary to add neither diurnal nor seasonal time information as separate input parameters. Also a variable coding the day of the week did not lead to an increased performance since F_c did not exhibit a distinct weekly cycle.

The described procedure was accomplished as a separate step in this paper to test the performance of ANN gap-filling with RBF. Therefore the mean values presented in Figs. 4–8 are based on the original dataset *with* gaps. Whenever sums of CO_2 exchange are reported (Section 3.4, Figs. 9 and 10) the results have been calculated from the gap-filled data.

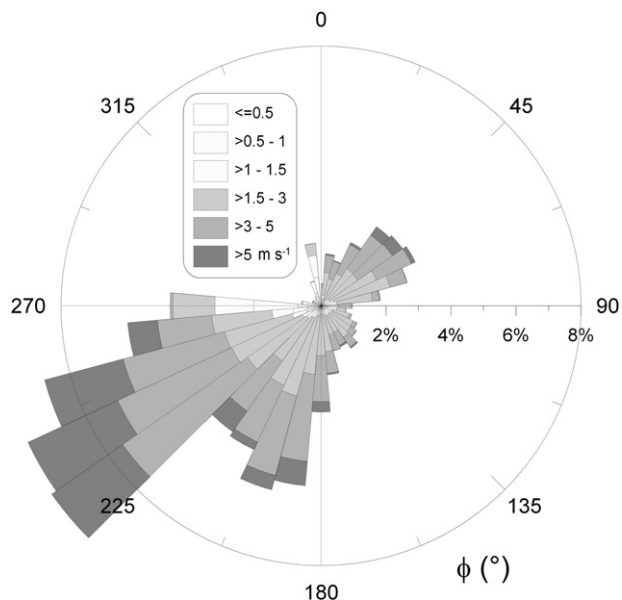


Fig. 3. Relative wind frequency distribution at the tower site GRT (26 m agl) in the study period from September 2006 to October 2007. Data is binned into 10° -classes.

3. Results and discussion

3.1. Meteorological situation during the study period

For a general characterisation of meteorological conditions during the measuring period monthly averages of meteorological quantities are depicted in Fig. 2. The average air temperature at GRK during the study period was 12.3°C while the precipitation sum (HSW) was 1029 mm. Both variables were elevated in comparison to the long term average for a comparable 14 month period at the German weather service station in Essen ($t_a = 10.0^\circ\text{C}$, $P = 962$ mm, period 1961–1990; Müller-Westermeier, 1996).

The reason for the extraordinary mild and wet conditions was an increased occurrence of cyclonic pressure systems with predominantly strong south-westerly winds and high precipitation

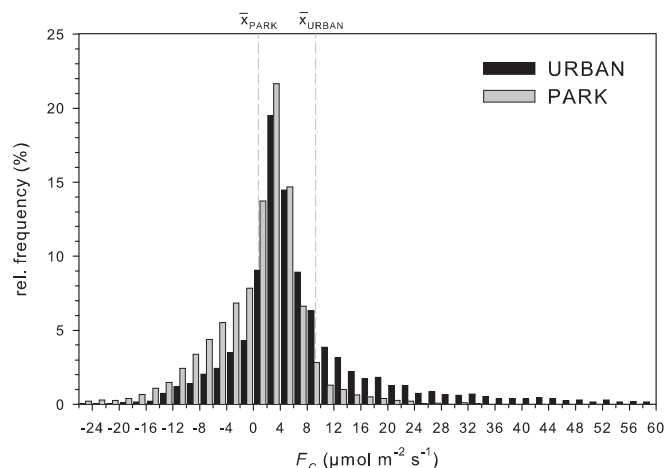


Fig. 4. Frequency distribution of F_c binned into classes of $2\ \mu\text{mol m}^{-2}\text{s}^{-1}$ during the study period from September 2006 to October 2007 for sectors with wind direction from $0^\circ < \phi \leq 180^\circ$ (urban) and $180^\circ < \phi \leq 270^\circ$ (park) respectively. The shown range $-24 < F_c < 60\ \mu\text{mol m}^{-2}\text{s}^{-1}$ accounts for 98% of all data. The vertical lines indicate the means of F_c for the park sector ($0.81\ \mu\text{mol m}^{-2}\text{s}^{-1}$) and the urban sector respectively ($9.29\ \mu\text{mol m}^{-2}\text{s}^{-1}$).

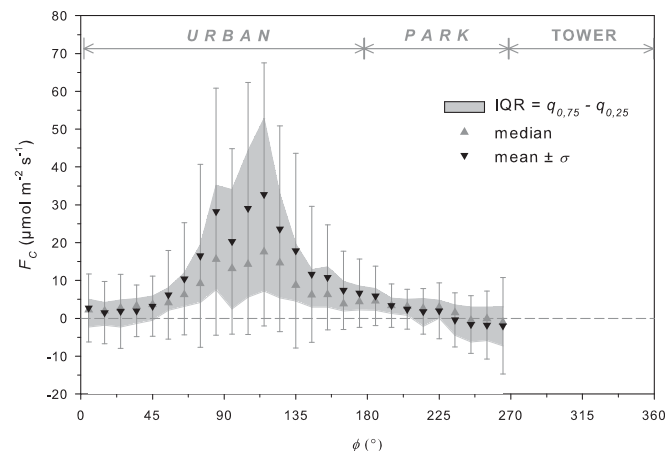


Fig. 5. Mean, median and the inter-quartile range (IQR) of F_c vs. wind direction (ϕ) binned into 10° -classes during the study period from September 2006 to October 2007.

particularly during the winter months 2006/07 and July–September 2007 (Fig. 2d). It is noticeable that January 2007 was solely characterised by these synoptic patterns. This month was extraordinary mild and wet ($4.6\ \text{K}$ and $34\ \text{mm}$ over the long term averages).

The wind frequency distribution at GRT shows the general prevailing of south-westerly winds (Fig. 3). Directions with $180^\circ < \phi \leq 270^\circ$ (park sector) occurred in 68.7% of the study period whereas winds out of the urban sector ($0^\circ < \phi \leq 180^\circ$) had a frequency of only 31.3% with generally lower wind speeds. A secondary maximum within this sector is visible with north-easterly winds. Winds from the north–west usually are rare in the region (6.1%).

3.2. Footprint modeling

For a better interpretation of fluxes measured at the tower site, footprint calculations have been performed with the model by Schmid (FSAM; Schmid, 1994). As initialising values, measuring height agl was used along with the aerodynamic roughness lengths and mean values for lateral turbulence intensity (σ_v/u^*) which were gained from the measurements (Table 3). In order to get an indication for an average area contributing to the flux, calculations were carried out for neutral atmospheric stability. An analysis of frequency of stability showed that 51% of the study period were characterised by neutral conditions ($-0.05 < \zeta < 0.05$; with $\zeta = (z-d)/L$, cf. Weber and Kordowski, in press). Under these circumstances an area with a radius of 1 km around the tower contributes to 80% of the flux according to the model initialised with a value of $\zeta = -0.05$.

This demonstrates that fluxes measured during approaching flow from south-western directions are predominantly influenced by the park area (see Fig. 1) while fluxes from the east and north–east have an urban footprint. Although there are slightly differences in z_0 and σ_v/u^* between the two land-use sectors, size and form of the source area function do not differ significantly between urban and park sector. In both cases the maxima of the modelled source functions are situated at $\approx 200\ \text{m}$ distance to the tower.

3.3. Magnitude of fluxes

In order to get an impression about the general statistical characteristics of CO_2 fluxes during the study period the frequency distribution of F_c is depicted in Fig. 4, again divided into urban and park sector. As expected, negative fluxes were found to occur more

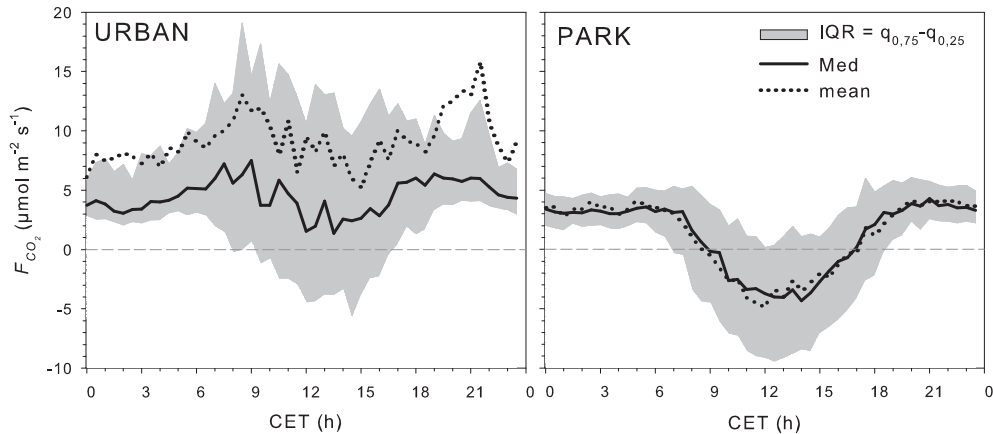


Fig. 6. Diurnal cycles of F_c (mean and median) during the entire study period from September 2006 to October 2007 for sectors with wind direction from $0^\circ < \phi \leq 180^\circ$ (*urban*) and $180^\circ < \phi \leq 270^\circ$ (*park*) respectively. The shaded area indicates the inter-quartile range (IQR), i.e. 50% of the data between the $q_{0.25}$ and $q_{0.75}$ quartiles.

frequently when the park area contributed to the footprint, showing moments of net CO₂ uptake by the park vegetation. Positive fluxes were measured with higher frequency with winds coming from the *urban* sector, however, a distinct fraction (27%) of these values were found to be negative, too. This gives first evidence for the photosynthetic activity of vegetation in parts of this sector as well.

In general, the dataset is characterised by a strong positive kurtosis, i.e. most of the measured fluxes are concentrated in a narrow range and the frequency decreases rapidly to higher absolute flux rates. For instance, over 20% of the data belongs to the class $2 < F_c < 5 \mu\text{mol m}^{-2} \text{s}^{-1}$ while the inter-quartile range (IQR, i.e. the central half of the data) only spans from -0.94 to $5.87 \mu\text{mol m}^{-2} \text{s}^{-1}$.

Based on the values of the non-gap-filled data the total average of F_c was $4 \mu\text{mol m}^{-2} \text{s}^{-1}$; with a higher mean for the *urban* ($9.3 \mu\text{mol m}^{-2} \text{s}^{-1}$) than for the *park* sector ($0.8 \mu\text{mol m}^{-2} \text{s}^{-1}$) which demonstrates that the city area is a considerable source of CO₂. But also the slight positive average of the *park* sector fluxes show that there is no net carbon transport to the surface on an annual basis. This is likely to be caused by CO₂ emitters within the park area (traffic on a single road crossing the park; maintenance activities). Taking the modelled footprint into account, areas beyond the park to the SW may contribute to the flux to some extent as well. However, these areas are of suburban ‘garden city’ and forest characteristics and are not considered to be strong source areas.

A detailed analysis of the dependency of F_c on wind direction is shown in Fig. 5. Here a considerable peak becomes evident in the

wind direction range $60^\circ < \phi \leq 100^\circ$ with high scattering due to the frequent occurrence of extremely high positive fluxes (maximum single 30 min flux: $135 \mu\text{mol m}^{-2} \text{s}^{-1}$). This results in a positive deviation of the class medians from the arithmetic means.

Wind directions out of the *park* sector show significantly lower absolute fluxes, averages of the sector with the longest park fetch ($230^\circ < \phi \leq 270^\circ$) exhibit weak negative fluxes. Also lower (positive) fluxes with a reduced scatter can be seen during winds coming from the north–west. This effect can be explained with the prevailing land-use in this sector: The north–east of the tower is characterised by only medium density residential areas with a high level of urban vegetation cover (road trees, gardens). In addition, a small park-like public green space pervades this neighbourhood (cf. Fig. 1). The low positive fluxes give evidence for an offsetting of emissions due to the urban vegetation, concurrently the emissions are reduced inherently by means of the low traffic density on the minor roads in this area.

Generally the fluxes of carbon dioxide are comparable to other urban sites with similar surroundings, e.g. in Helsinki (Vesala et al., 2008a) or Basel (Vogt et al., 2006) however the scatter is considerably higher. Although differences in land-use around tower sites have been reported to be retraceable in flux magnitudes (Edinburg, Nemitz et al., 2003; Melbourne, Coutts et al., 2007), in this study larger differences depending on the direction of approaching flow were visible. This was expected with regard to the influence of the park vegetation and can also be attributed to the unevenly distributed sources of CO₂ around the tower.

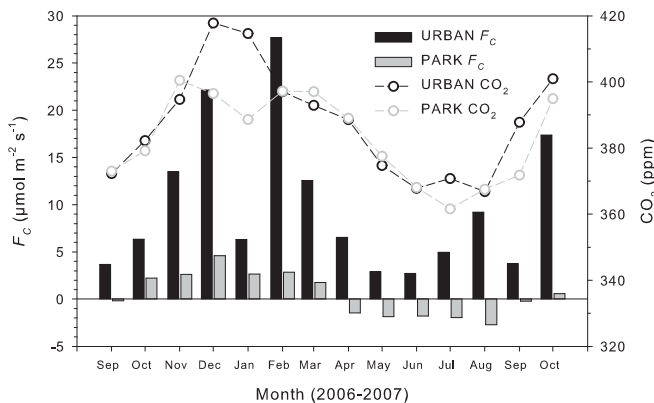


Fig. 7. Monthly averages of F_c and CO₂ mixing ratios for sectors with wind direction from $0^\circ < \phi \leq 180^\circ$ (*urban*) and $180^\circ < \phi \leq 270^\circ$ (*park*) respectively.

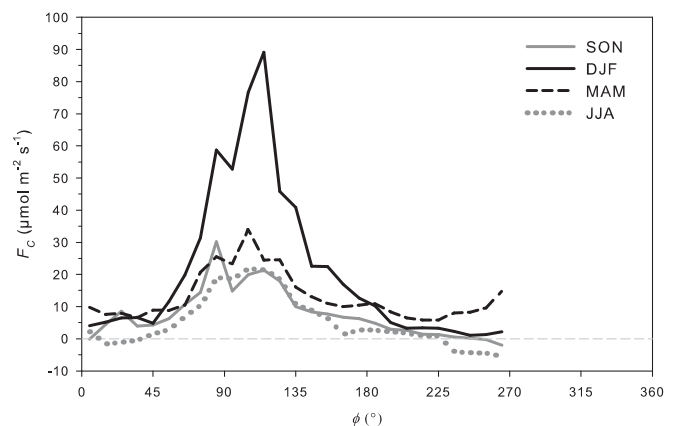


Fig. 8. Seasonal averaged values of F_c vs. wind direction, binned into 10° -classes.

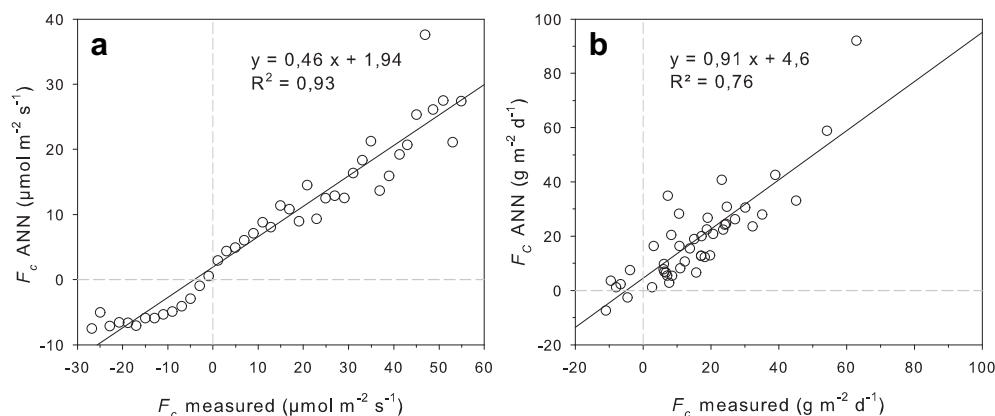


Fig. 9. Linear regressions between a) measured and ANN modelled 30-min F_c (binned into classes of $2 \mu\text{mol m}^{-2} \text{s}^{-1}$, 98% of data is shown); b) daily sums of F_c measured at 46 days during the study period when no data gaps occurred and the corresponding sums calculated from the ANN results.

3.4. Diurnal and annual variability of carbon dioxide fluxes

Both, biogenic and anthropogenic forcings which influence the release and uptake of carbon dioxide vary over time on the diurnal and annual scale. The diurnal variability of F_c is depicted in Fig. 6, again divided into the both land-use sectors. Fluxes out of the *park* sector appeared to be clearly governed by plant activity with negative daytime fluxes (with a maximum uptake of $-4 \mu\text{mol m}^{-2} \text{s}^{-1}$ on average) while night-time fluxes remained positive but constant due to CO_2 release by respiration processes. Similar cycles of F_c have been described for non-urban forest sites (Goulden et al., 1996; Papale et al., 2006; Schindler et al., 2006) even though noon maxima uptake rates may vary between different sites.

The average temporal evolution of the *urban* sector fluxes confirms the impact of anthropogenic emissions. Maximum fluxes occurred during the morning rush hour, though a clear signal of the daily traffic variability cannot be seen due to the high scattering, neither in the diurnal cycle nor in the weekday/weekend comparison (not shown here). Despite the fact, that the mean and median values are positive throughout the day, there have been situations with a net transport to the surface during noon and afternoon hours in the *urban* sector as well. These were mainly related to spring and summer conditions with winds coming from the

north-east and can be explained with the carbon uptake by the urban vegetation within the low density residential neighbourhood situated there (see above).

The general influence of land-use around the tower also becomes apparent in the seasonal variation (Figs. 7 and 8). Based on monthly averages the onset of net carbon uptake for the *park* sector in 2007 occurred in April and the maximum was reached in August. The mean flux then remained negative until October which corresponds to the extent of the thermal vegetation period in this year (daily mean $t_a > 10^\circ \text{C}$ from April 9 to October 10).

For the *urban* sector maximum emissions of CO_2 could be observed in the winter months except for January 2007 in which the area of the flux footprint was mainly situated over the park. Meteorological conditions in this month were mainly characterised by strong cyclonic systems with high wind speeds from SW. The accompanying strong atmospheric mixing may also explain the lower CO_2 concentrations in this month (Fig. 7). The annual evolution of wind direction dependency (Fig. 8) gives further evidence that the magnitude of CO_2 emissions from the urban sector were mainly driven by domestic heating (mainly natural gas burning within the study area) in winter (DJF) and remains stable throughout the rest of the year to a greater or lesser extent, which can be attributed to road traffic emissions.

Flux differences between winter and summer seasons in the order of two third, as they appear in this study, have also been observed during a one-year period in Copenhagen (Soegaard and Møller-Jensen, 2003). There, the annual variability of F_c also was attributed mainly to variations in heating emissions.

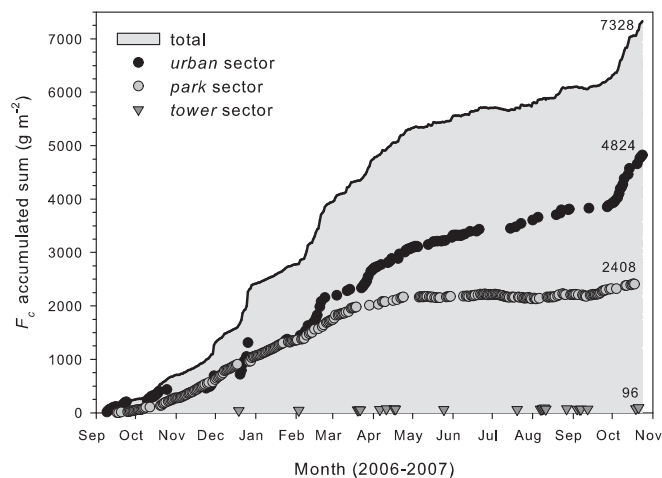


Fig. 10. Accumulated daily sums of F_c during the 411 days of the study period based on the ANN gap-filled measured data (shaded area). The single symbols denote the corresponding subtotals for the different wind direction sectors. The numbers on the right hand give the total sums for each graph.

3.5. Gap-filled cumulative fluxes

As mentioned above (2.2), it was sufficient to use wind direction, temperature and solar radiation for the chosen RBF network to reproduce F_c with a minimal error. In particular, the pronounced dependency of F_c on wind direction at the given site led to a high sensitivity of the model to this parameter. Furthermore, temperature and solar radiation have an instantaneous impact on biological processes by steering photosynthetic activity and respiration of the biosphere.

An analysis of fluxes out of the tower sector ($270^\circ > \phi \geq 360^\circ$) on integral turbulence characteristics and stationary conditions of $w'\rho_c^{-1}$ (Foken and Wichura, 1996) exhibited the data to be of sufficient quality. For the reason that the ANN gap-filling for the entire sector would not have led to a higher overall quality level, the measured flux data of this sector was adjoined to the dataset again.

Table 4

Parameters used for artificial neural network inputs and characteristics of the networks' performance in the reproduction of F_c and ρ_c . In the case of F_c wind direction was used in form of four fuzzy values ϕ_{fx} , each indicating the percentage of the four directions x (N, E, S, W) to the actual wind direction. Topology denotes the number of neurons in the input, hidden and output layers, r is coefficient of correlation between measured and modelled values, $RMSE$ is the root mean square error.

	F_c	ρ_c
Input parameters	$\phi_{fN}, \phi_{fE}, \phi_{fW}, t_s, S_d$	$U, \phi, \overline{w^2}, t_s, S_d$
Network type	RBF	RBF
Topology	5-189-1	5-462-1
r	0,68	0,83
$RMSE$	$8.64 \mu\text{mol m}^{-2} \text{s}^{-1}$	0.45mmol m^{-3}

The use of RBF networks for both, the reproduction of F_c and ρ_c (Table 4) turned out to be superior to MLP networks, as it was shown in Schmidt et al. (2008) before. However, in the present dataset the performance of reproducing the time series of F_c was weakened by the large variability of the fluxes while the modeling of ρ_c worked more satisfactorily (further results not shown here). A key problem rose from high absolute fluxes in both, the positive and negative range ($|F_c| > 20 \mu\text{mol m}^{-2} \text{s}^{-1}$) which were not sufficiently replicated by the ANN. This resulted in a general underestimation of F_c by the network (Fig. 9a).

On the contrary, the actual purpose of performing a gap-filling procedure is to sum surface-atmosphere exchanges of carbon dioxide. This was tested with a comparison of daily sums of F_c and the correspondent ANN results of these days on which gapless measurements were available. In doing so, the overall performance of the flux modeling by means of ANN generalisation can be assessed as being satisfactorily (Fig. 9b).

Finally, daily sums have been calculated from the gap-filled dataset in which the ANN data accounted for 36.2% of the dataset (cf. 2.1). The accumulation over all 411 days of the research period is depicted in Fig. 10. While the average daily source strength was $17.8 \text{g CO}_2 \text{m}^{-2} \text{d}^{-1}$, highest emission rates occurred during the fall and winter months (maximum $261.7 \text{g m}^{-2} \text{d}^{-1}$). January 2007 exhibits an episode of weakened positive transport of CO_2 into the atmosphere which is related to the exceptional mild meteorological conditions during this month with predominant winds from the park sector. During the summer months of 2007 episodes are visible where the accumulation exhibits a stagnating or weak declining course. Splitting the daily sums into the above used sectors by considering the mean daily wind direction it becomes evident that negative daily sums of F_c are solely related to the park sector (maximum daily uptake $-22.7 \text{g m}^{-2} \text{d}^{-1}$) while the slope of the urban sum is positive all the time.

Reducing the examined period to the length of exactly one year (October 2006 up to and including September 2007) a comparable yearly sum of $6031 \text{g m}^{-2} \text{a}^{-1}$ is resulting. Although it must be taken into account that park sector fluxes were prevailing during the study period this sum is in the same order of magnitude as results reported the suburban site in Melbourne ($8490 \text{g m}^{-2} \text{a}^{-1}$; Coutts et al., 2007) but is considerable lower than yearly emissions from densely built-up sites in Mexico City ($12,800 \text{g m}^{-2} \text{a}^{-1}$; Velasco et al., 2005) or Tokyo ($12,302 \text{g m}^{-2} \text{a}^{-1}$; Moriwaki and Kanda, 2004).

4. Summary and conclusions

Turbulent fluxes of carbon dioxide have been measured for a period of nearly 14 month over an urban park area to assess the temporal evolution on the diurnal and seasonal scale. It was possible to assign patterns in flux variability to the prevailing land-use properties within the flux footprint, i.e. whether vegetation or traffic/built-up areas contributed to the exchange of carbon

dioxide. Urban fluxes were mainly governed by anthropogenic emissions whereas domestic heating seemed to be the more considerable source in winter. Although traffic related CO_2 production led to positive daytime fluxes on average during summer, around noon an offsetting to lower positive values was visible due to carbon uptake by the urban vegetation, i.e. road trees, gardens and public green spaces within the urban landscape.

On the opposite, fluxes with a park footprint exhibited pronounced biogenic features with negative daytime fluxes and constant release of CO_2 due to respiration at night. Although the park and the surrounding forest patches are temporary local carbon sinks, the area was a weak source of CO_2 over the entire year. This can be attributed to the low but existent anthropogenic emissions from the single road crossing the area and from maintenance activities in the park (lawn mowing, gardening).

Taking the whole site into account, the surface turned out to be a considerable source of CO_2 with an annual release of $6031 \text{g m}^{-2} \text{a}^{-1}$. Thus, the presence of local sinks embedded into the urban environment is only able to offset anthropogenic emissions to a certain extent.

The chosen gap-filling procedure by means of artificial neural network generalisation worked satisfyingly for reproducing daily sums. In future urban applications this approach needs further non-meteorological inputs which are related to the flux variability (e.g. real time data of traffic density and gas consumption) in order to gain a reliable time series reconstruction.

In conclusion, it turns out that carbon exchange processes over urban areas are not only governed by anthropogenic emissions but also are influenced by biogenic activity, certainly depending on the local surface properties. In order to gain more information about a larger number of urban land-use types further measurements are required.

Acknowledgements

Thomas Hanster (Grugapark, Essen) is acknowledged for providing permission to install the measurement instrumentation at the tower. The sonic anemometer was provided by Prof. Konradin Weber (University of Applied Sciences, Düsseldorf) which is highly appreciated. Thanks to the technical assistance by Andreas Schmidt and Markus Nekes for installing and maintaining the measurement equipment.

References

- Baldocchi, D., Gu, L., Goldstein, A., Falge, E., Olson, R., Hollinger, D., Evans, R., Running, S., Anthoni, P., Law, B., Bernhofer, C., Davis, K., Fuentes, J., Katul, G., Lee, X., Malhi, Y., Meyers, T., Wilson, H., Munger, W., Wofsy, S., Oechel, E., Pux, U.K.T., Pilegaard, K., Schmid, H.P., Valentini, R., Verma, S., Vesala, T., 2001. FLUXNET: a New tool to study the temporal and spatial variability of ecosystem-scale carbon dioxide, water vapor, and energy flux densities. *Bulletin of the American Meteorological Society* 82, 2415–2434.
- Baldocchi, D., 2003. Assessing the eddy covariance technique for evaluating carbon dioxide exchange rates of ecosystems: past, present and future. *Global Change Biology* 9, 479–492.
- Baldocchi, D., 2008. TURNER REVIEW No. 15. 'Breathing' of the terrestrial biosphere: lessons learned from a global network of carbon dioxide flux measurement systems. *Australian Journal of Botany* 56, 1–26.
- Coutts, A.M., Beringer, J., Tapper, N.J., 2007. Characteristics influencing the variability of urban CO_2 fluxes in Melbourne, Australia. *Atmospheric Environment* 41, 51–62.
- Falge, E., Baldocchi, D., Olson, R., Anthoni, P., Aubinet, M., Bernhofer, C., Burba, G., Ceulemans, R., Clement, R., Dolman, H., Granier, A., Gross, P., Grünwald, T., Hollinger, D., Jensen, N., Katul, G., Keronen, P., Kowalski, A., Lai, C.T., Law, B.E., Meyers, T., Moncrieff, J., Moors, E., Munger, J.W., Pilegaard, K., Rannik, Ü., Rebmann, C., Suyker, A., Tenhunen, J., Tu, K., Verma, S., Vesala, T., Wilson, K., Wofsy, S., 2001. Gap filling strategies for defensible annual sums of net ecosystem exchange. *Agricultural and Forest Meteorology* 107, 43–69.
- Foken, T., Wichura, B., 1996. Tools for quality assessment of surface-based flux measurements. *Agricultural and Forest Meteorology* 78, 83–105.

- Goulden, M.L., Munger, J.W., Fan, S.M., Daube, B.C., Wofsy, S.C., 1996. Measurements of carbon sequestration by long-term eddy covariance: methods and a critical evaluation of accuracy. *Global Change Biology* 2, 169–182.
- Grimmond, C., Oke, T., 1999. Aerodynamic properties of urban areas derived from analysis of surface form. *Journal of Applied Meteorology* 38, 1262–1292.
- Grimmond, C.S.B., King, T., Cropley, F., Nowak, D., Souch, C., 2002. Local-scale fluxes of carbon dioxide in urban environments: methodological challenges and results from Chicago. *Environmental Pollution* 116, 243–254.
- Grimmond, C.S.B., Offerle, B., Salmond, J.A., Oke, T.R., Lemonsu, A., 2004. Flux and turbulence measurements at a densely built-up site in Marseille: heat, mass (water and carbon dioxide), and momentum. *Journal of Geophysical Research D: Atmospheres* 109, 1–19.
- Kaimal, J.C., Finnigan, J.J., 1994. *Atmospheric Boundary Layer Flows – Their Structure and Measurements*. Oxford University Press, New York, Oxford, 285 pp.
- Liu, H., Peters, G., Foken, T., 2001. New equations for sonic temperature variance and buoyancy heat flux with an omnidirectional sonic anemometer. *Boundary-Layer Meteorology* 100 (3), 459–468.
- Matese, A., Gioli, B., Vaccari, F.P., Zaldei, A., Miglietta, F., 2009. Carbon dioxide emissions of the City Center of Firenze, Italy: measurement, evaluation, and source partitioning. *Journal of Applied Meteorology and Climatology* 48 (9), 1940–1947.
- McPherson, E.G., 1998. Atmospheric carbon dioxide reduction by sacramento's urban forest. *Journal of Arboriculture* 24, 215–223.
- Moffat, A.M., Papale, D., Reichstein, M., Hollinger, D.Y., Richardson, A., Barr, A.G., Beckstein, C., Braswell, B.H., Churkina, G., Desai, A.R., Falge, E., Gove, J.H., Heimann, M., Hui, D., Jarvis, A., Kattge, J., Noormets, A., Stauch, V.J., 2007. Comprehensive comparison of gap-filling techniques for eddy covariance net-carbon fluxes. *Agricultural and Forest Meteorology* 147, 209–232.
- Moore, C.J., 1986. Frequency response corrections for eddy correlation systems. *Boundary-Layer Meteorology* 37 (1–2), 17–35.
- Moriwaki, R., Kanda, M., 2004. Seasonal and diurnal fluxes of radiation, heat water vapor, and carbon dioxide over a suburban area. *Journal of Applied Meteorology* 43, 1700–1710.
- Müller-Westermeier, G., 1996. *Klimadaten von Deutschland. Zeitraum 1961–1990*. Selbstverlag des Deutschen Wetterdienstes, Offenbach am Main.
- Nemitz, E., Hargreaves, K.J., McDonald, A.G., Dorsey, J.R., Fowler, D., 2002. Micro-meteorological measurements of the urban heat budget and CO₂ emissions on a city scale. *Environmental Science and Technology* 36 (14), 3139–3146.
- Nowak, D.J., Crane, D.E., 2002. Carbon storage and sequestration by urban trees in the USA. *Environmental Pollution* 116, 381–389.
- Papale, D., Reichstein, M., Aubinet, M., Canfora, E., Bernhofer, C., Kutsch, W., Longdoz, B., Rambal, S., Valentini, R., Vesala, T., Yakir, D., 2006. Towards a standardized processing of Net Ecosystem Exchange measured with eddy covariance technique: algorithms and uncertainty estimation. *Biogeosciences* 3, 571–583.
- Papale, D., Valentini, R., 2003. A new assessment of European forests carbon exchanges by eddy fluxes and artificial neural network spatialization. *Global Change Biology* 9 (4), 525–535.
- Ptak, D., Kuttler, W. Near Surface CO₂-Concentrations in two north-west German Cities with different topography, submitted for publication.
- Schindler, D., Türk, M., Mayer, H., 2006. CO₂ fluxes of a Scots pine forest growing in the warm and dry southern upper Rhine plain, SW Germany. *European Journal of Forest Research* 125, 201–212.
- Schmid, H.P., 1994. Source areas for scalars and scalar fluxes. *Boundary-Layer Meteorology* 67, 293–318.
- Schmid, H.P., 2002. Footprint modeling for vegetation atmosphere exchange studies: a review and perspective. *Agricultural and Forest Meteorology* 113, 159–183.
- Schmidt, A., Wrzesinsky, T., Klemm, O., 2008. Gap filling and quality assessment of CO₂ and water vapour fluxes above an urban area with radial basis function neural networks. *Boundary-Layer Meteorology* 126, 389–413.
- Soegaard, H., Møller-Jensen, L., 2003. Towards a spatial CO₂ budget of a metropolitan region based on textural image classification and flux measurements. *Remote Sensing of Environment* 87, 283–294.
- Svirejeva-Hopkins, A., Schellnhuber, H.J., Pomaz, V.L., 2004. Urbanised territories as a specific component of the Global Carbon Cycle. *Ecological Modelling* 173, 295–312.
- UN-Habitat, 2006. *State of the World's Cities 2006/2007. The Millennium Development Goals and Urban Sustainability*. UN-Habitat, Nairobi, 204 pp.
- Velasco, E., Pressley, S., Allwine, E., Westberg, H., Lamb, B., 2005. Measurements of CO₂ fluxes from the Mexico City urban landscape. *Atmospheric Environment* 39, 7433–7446.
- Vesala, T., Jarvi, L., Launiainen, S., Sogachev, A., Rannik, U., Mammarella, I., Siivola, E., Keronen, P., Rinne, J., Riikonen, A., Nikinmaa, E., 2008a. Surface-atmosphere interactions over complex urban terrain in Helsinki, Finland. *Tellus, Series B: Chemical and Physical Meteorology* 60 B, 188–199.
- Vesala, T., Kljun, N., Rannik, U., Rinne, J., Sogachev, A., Markkanen, T., Sabelfeld, K., Foken, T., Leclerc, M.Y., 2008b. Flux and concentration footprint modelling – state of the art. *Environmental Pollution* 152, 653–666.
- Vogt, R., Christen, A., Rotach, M.W., Roth, M., Satyanarayana, A.N.V., 2006. Temporal dynamics of CO₂ fluxes and profiles over a Central European city. *Theoretical and Applied Climatology* 84 (1–3), 117–126.
- Webb, E.K., Pearman, G.I., Leuning, R., 1980. Correction of flux measurements for density effects due to heat and water vapour transfer. *Quarterly Journal Royal Meteorological Society* 106, 85–100.
- Weber, S., Kordowski, K., Comparison of atmospheric turbulence characteristics and turbulent fluxes from two urban sites in Essen, Germany. *Theoretical and Applied Climatology*, in press, doi:10.1007/s00704-009-0240-8.